



An optimal deployment scheme for extremely fast charging stations

Ping Zhong¹ · Aikun Xu¹ · Yilin Kang² · Shigeng Zhang¹ · Yiming Zhang³

Received: 20 October 2021 / Accepted: 17 February 2022

© The Author(s), under exclusive licence to Springer Science+Business Media, LLC, part of Springer Nature 2022

Abstract

Electric vehicles (EVs) are important for most countries and regions that rely on imported energy. Unfortunately, slow recharge and improper deployment at charging stations have limited the widespread use of EVs. To improve the recharging speed of charging stations and optimize their deployment, we propose a Minimized optimization Deployment algorithm based on EV Dynamic Changes (MDDC) to optimize the deployment of eXtremely Fast Charging (XFC) stations. The method selects multiple EV distribution maps to simulate EV movement and utilizes a grid partitioning method to divide the deployment area. To reduce the deployment scope of XFC stations, the grids with small and stable EV numbers variance are excluded from service areas. Then, we design the minimum required XFC station optimization function to achieve coverage for all EVs. Three optimization rules are designed to reduce the overlapping coverage of XFC stations, which minimizes the number of XFC stations. Finally, we use an efficient and accurate method named Minimum dIstance Sum of Unique Public area location (MISUP) in MDDC to redetermine the deployment location of XFC stations. We verify the rationality, effectiveness, and robustness of MDDC through extensive simulations, and the results show that the MDDC outperforms the comparison algorithm by 54.2% and 52.0% when using the Euclidean algorithm and the A-star algorithm, respectively.

Keywords Electric vehicle · Extremely fast-charging station · Facility deployment · Charging infrastructure · Planning

1 Introduction

Fossil fuels are nonrenewable energy sources that play a vital role in the development of cities. Unfortunately, these energy sources will eventually run out over time [1, 2]. Most countries and regions that rely on imported fossil fuels

have an urgency to find alternative energy sources. Electricity is a renewable energy source with clean characteristics, so it is considered the most ideal alternative to fossil fuels. Transportation using electricity as an energy source is becoming more and more popular, especially Electric Vehicles (EVs). As far as we know, EVs can reduce emissions that cause climate change and smog, thus achieving the goal of improving the environment and public health [3]. Therefore, replacing internal combustion engine vehicles with EVs in traditional transportation networks has gradually become a new trend [4–6]. The EV Charging Station (EVCS or CS) plays an important role in the operation and development of EVs [7]. However, the traditional CS (i.e., fast charging (< 150 kW)) diverges between the time required to fully charge the EVs and the needs of the EV user, which severely limits the widespread use of EVs [8, 9]. Recently, the industry has addressed the slow charging problem of EVs with eXtremely Fast Charging (XFC) (> 350 kW) [10–12], which also known as ultra-fast direct-current fast chargers, is currently not commercially available and is expected to become a standard configuration in the future [3]. The XFC station is an infrastructure that provides XFC services for EVs at CS.

✉ Shigeng Zhang
sgzhang@csu.edu.cn

Ping Zhong
ping.zhong@csu.edu.cn

Aikun Xu
aikunxu@csu.edu.cn

Yilin Kang
ylkang@mail.scuec.edu.cn

Yiming Zhang
zhangyiming@nudt.edu.cn

¹ School of Computer Science and Engineering, Central South University, Changsha 410083, China

² School of Computer Science, South Central University for Nationalities, Wuhan 430074, China

³ School of Computer, National University of Defense Technology, Changsha 410073, China

Compared with internal combustion engine vehicles, EVs will take longer to replenish energy at CS, but travel less. Due to the limited travel range, EVs may need to recharge batteries when users travel to far destinations. Therefore, users care about the convenience of EV charging very much, which plays an important role in the promotion and popularization of EVs. CS owners have to install enough XFC stations for users. However, the large-scale deployment of XFC stations will not only lead to higher land occupation rates but also increase the energy company's investment costs and the burden of urban development. Therefore, minimizing the number of required XFC stations is important for energy companies and governments. After determining the number of XFC stations, how to deploy the XFC stations so that they can serve as many EVs as possible is an optimization problem.

The optimal deployment of charging stations has been a research topic in both industry and academia [13]. Researchers have conducted many studies in the field of EV charging station deployment based on different optimization goals. Many works have analyzed from the perspectives of economic benefits [14–16] and grid factors [17–19]. Other works have typically focused on specific issues. For example, Zhao et al. [18] adopted a modified huff gravity-based model to describe the probabilistic patronizing behaviors of EV users. This work also formulated a bilevel optimization model to decide the optimal site and size of the charging station. Luo et al. [20] modeled the EV charging industry as an oligopolistic market. The best placement strategy is obtained through interaction in Bayesian games without the size issue. Wang et al. [2] attempted to find the best path to charge a long working bus with and without considering a limited battery size. Similarly, Wu et al. [21] also designed a solution for the bus. However, it is still very important to study the deployment of charging stations.

In this paper, we study the deployment of charging stations from the perspective of EV data dynamics. To solve a low utilization rate, high initial investment cost, and high land occupation rate when deploying XFC stations, a Minimized optimization Deployment algorithm based on EV Dynamic Changes (MDDC) is proposed. The main contributions of our work are as follows:

- For the changing position of EVs, we first use multiple EV distribution maps to approximate the moving process of EV. Then, the grid partition method is used to divide the EV distribution map into multiple subgrids, and the average and the variance of EVs in the subgrid are calculated. A type of grid with a larger average number of EVs and smaller variances are retained as key regions, thereby achieving large-scale coverage and high stability of key regions.

- The minimum required XFC station optimization function with a heuristic algorithm is designed to achieve coverage for all EVs in the service area of the XFC station. According to the driving range of EVs, three optimization rules in the same clique are designed to reduce overlap between the service areas to achieve the optimal deployment of the XFC stations.
- The MDDC method is proposed to minimize the number of required XFC stations for optimal deployment. To improve the utilization of the XFC station and user satisfaction, an efficient and accurate method named the Minimum dIstance Sum of Unique Public area location (MISUP) is designed in MDDC to redetermine the location of the XFC stations. Additionally, we verify the validity and rationality of the MDDC and evaluate its performance.

The rest of this paper is organized as follows. Section 2 describes the related work. Section 3 describes the methodology. Section 4 presents the simulation results. Section 5 concludes the paper.

2 Related work

Over the past few years, with the reduction of nonrenewable energy sources such as fossil fuels, minerals, and nuclear fuels. An increasing number of countries and regions in the world have encouraged industrial [22–25] and academic circles [26–31] to find and use renewable energy sources (e.g., Singapore [1], Greece [8], and China [32]). The search for new renewable energy sources become a research topic of interest. EVs are often identified as the most promising technology to enable the decarbonization of transportation. Researchers have made many efforts to advance the use of EVs [30, 33]. However, solving the charging problem is the key to promoting EVs. Therefore, the deployment of the charging station is one of the most important topics worth studying. There are some works studying charging station placement with different views.

EV users play an important role in the deployment of the charging station. Zhu et al. [34] proposed a new model of plug-in electric vehicle charging station planning considering users' daily travel patterns. The model aimed at the cost of the charging station and the user habits, which could simultaneously handle the problems of positioning the charging station and determining how many chargers should be established at each charging station. In addition, this work also studied the impact of different discount rates, charging station operating cycles, the number of electric vehicles, and the number of charging stations at the locations. Alhazmi et al. [35] considered both the trip success ratio and driving preferences in a model to enhance the accessibility of

plug-in electric vehicle CSs. The CS placement problem was transformed into a Maximum Covering Location Problem (MCLP) to determine the best deployment location for CSs. However, this work ignored the economic factors affecting the choice of CS. Li et al. [36] proposed and implemented a new algorithm for evaluating charging needs and planning new charging stations. In addition, modeling and analysis of charging-related search behaviors, navigation behaviors, and charging station usage patterns were performed. To evaluate the charging demand, a Bayesian inference algorithm was proposed to fuse these three behaviors. In addition, a flexible objective function was proposed to serve existing EV users and attract more FFV users. Luo et al. [20] studied the multistage deployment of CSs based on the increase in EV penetration. A nested logit model was used to analyze the preferences of EV users to integrate the needs of each CS to achieve their optimal deployment. However, this work does not consider the size issue of CS.

In addition, the problem of solving the optimal deployment location of charging stations based on CS deployment costs, user costs, and grid costs has been widely studied. A method that can determine the location of the charging station and the optimal charging performance was proposed by Rajabi-Ghahnavieh et al. [37]. This work redefined the proposed problem as a Mixed-Integer Nonlinear Programming (MINLP) problem to reduce the total expected cost of EV charging. The charging demand and the expected cost of EV users were evaluated by considering user behavior. Then, the optimal CS deployment location was determined by zone division. However, this work did not consider the available space of the charging station before assigning candidate charging stations. The experiment in this work was carried out with a small area and a small number of EVs. We are still not sure whether the method would be effective in a large area with a large number of EVs. Moreover, this work did not fully consider the overlapping coverage between CS service scopes. Ge et al. [38] considered the network structure, distributed network system structure, and performance constraints in an optimization process. A weighted Voronoi diagram was used to divide the service area of the charging station while optimizing the performance of the charging station based on queuing theory. Finally, the optimal deployment of charging stations was achieved by minimizing total social benefits. However, the partition results were based on the initial EV distribution information, which cannot fully reflect the distribution of EVs. Sadeghi-Barzani et al. [39] proposed a mixed-integer nonlinear optimization algorithm that considered the cost of deploying the charging station, the EV energy loss, the grid loss, the substation location, and the urban road network to determine the location of fast-charging stations. Genetic Algorithm (GA) technology is used to solve these problems.

In addition, the impact of the reliability of the power grid on the location of the charging station was evaluated by using the loss of charging cost. However, this work did not consider dynamic changes in EV location.

Other views were often studied. Andrenacci et al. [22] proposed a strategy for optimizing the charging infrastructure of electric vehicles in urban areas. This strategy estimated the energy requirements of each sector from the perspective of the energy consumed by the equivalent EV fleet to reach the destination, which used data collected by traditional vehicles to solve the deployment optimization problem of EVCSs. However, the strategy did not consider city policies, distribution network conditions, and the potential location of the cluster centroid. He et al. [5] proposed a bilevel planning model that considered the driving range of an electric vehicle to find the optimal location of a charging station. However, the bilevel programming model was rarely applied to large networks due to its computational difficulty, and it was only suitable for testing on small networks. Similarly, Xiong et al. [1] also described the layout of charging stations as a bilevel planning problem to minimize social costs, in which the allocation of the optimal stations was determined by capturing the competitive and strategic behavior. Vazifeh et al. [23] proposed a modeling and optimization framework that could determine the effective deployment of charging stations to minimize the total energy consumption and the over-the-road driving distance from EV users to charging stations. However, this solution ignored factors such as load density, traffic density, and solution space closure. In addition to the above-mentioned shortcomings, these previous works also have the following situations. 1) Some works only consider the location of charging stations without considering the number of chargers [24–26, 37], while others only consider the number of chargers without considering the location of the charging stations [27–29]. None of these works can meet the needs of energy companies. 2) The obtained results created a serious overlap between the XFC station's service areas. 3) The positioning algorithms were often inefficient in the previous works.

3 Methodology

In this section, we try to solve the problem of the optimal deployment of XFC stations. The MDDC is proposed to solve this problem, which is shown in Algorithm 1. In the MDDC, we first use the grid partitioning method to divide the EV distribution map into subgrids, which can reduce the service range of the XFC station. In the following, we model the problem of minimizing the number of XFC station deployments and use heuristic algorithms to solve the problem. XFC station deployment location optimization

Algorithm 1 MDDC Algorithm**Algorithm 1** MDDC Algorithm

Input: EV data a , Period Ω , Time interval ξ
Output: $CSCS$: a set of charging station coordinates

1. $CSCS \leftarrow \emptyset$
2. $P_{important} \leftarrow \text{DeterminingArea}(a, \Omega, \xi)$
3. $G \leftarrow \text{MinimizingNum}(P_{important})$
4. $CSCS \leftarrow \text{Rule}(CSCS, G)$
5. $CSCS \leftarrow \text{MISUP}(CSCS)$
6. **return** $CSCS$
7. **function** $\text{DeterminingArea}(a, \Omega, \xi)$
8. $E(i) \leftarrow \text{Equation}(1)$ // the average value of EVs in grid i
9. $E_{mean} \leftarrow \text{Equation}(2)$ // the average value of EVs, exclude grid i when $E(i) < E_{mean}$
10. $S_i^2 \leftarrow \text{Equation}(3), S_i^2 \leftarrow \text{Ascending}(S_i^2)$ // calculate the variance of the EV of the grids i
11. **return** grid i // select the grid corresponding to the first L variances as the key areas
12. **function** $\text{MinimizingNum}(P_{important})$
13. $D \leftarrow \text{Equation}(4)$ // D consists of the EVs range in $P_{important}$
14. $x_j = \begin{cases} 1 & \text{if } D_j \text{ is the final deployment area} \\ 0 & \text{if } D_j \text{ is not the final deployment area} \end{cases}$ // $D_j \in D, x_j$ is the binary decision variable
15. $G_j = \text{argmin} \sum_{j=1}^{|D|} x_j$ // minimize the number of XFC stations deployed in the $P_{important}$
16. **return** G // update G_j, G , return G
17. **function** $\text{Rule}(CSCS, G)$
18. **if** $\text{sum}(UPA) == 0$ **do** // UPA is unique public area
19. $CSCS = CSCS \cup UPAC$ // $UPAC$ is public areas intersect coordinate
20. **else if** $\text{sum}(UPA) == 1$ **do**
21. $CSCS = CSCS \cup CUPAC$ // $CUPAC$ is the centroid of the unique public area coordinate
22. **else**
23. G is divided into two subsets $subG1$ and $subG2$, at least one with the UPA
24. $CSCS = \text{Rule}(CSCS, subG1)$
25. $CSCS = \text{Rule}(CSCS, subG2)$
26. **return** $CSCS$
27. **function** $\text{MISUP}(CSCS)$ // search area is UPA
28. **for** p from 0 to $\text{Len}(CSCS)$
29. $EVC \leftarrow \text{Query}(CSCS[p])$ // EVC is a list of EVs served by a charging station p
30. **if** $n < 2$ or $\text{sum}(UPA) < 2$ **do** // $EVC.x = \{x_1, x_2, \dots, x_n\}, EVC.y = \{y_1, y_2, \dots, y_n\}$
31. $CSCS[p] = CSCS[p]$ // $EVC.x$ and $EVC.y$ are the coordinates of EVs
32. **else**
33. $CSCS[p] = \text{argmin} \sum_{i=1}^n \sqrt{(x - x_i)^2 + (y - y_i)^2}$ // obtain (x, y)
34. **return** $CSCS$

rules within the same clique are introduced afterward to optimize XFC station deployment. In addition, to further improve user satisfaction and the utilization of the XFC station, we propose Minimum dIstance Sum of Unique Public area location (MISUP) in the MDDC to shorten the calculation time and accurately obtain the optimal deployment location of the XFC station.

3.1 Determining the best charging area for the XFC station

In this paper, the distribution map covers a large area in a real environment, so we assume that the number of electric vehicles in each distribution map is the same and their position is variable. During data processing, our goal is to determine the number and variance of EVs in each sub-grid. In Ω/ξ electric vehicle distribution maps within a period Ω selected with ξ as the time interval, we use the grid partitioning method to narrow the area of the XFC station service area. The total area is represented by $R = \{b_1^1, \dots, b_1^{\theta}, \dots, b_{\Omega/\xi}^1, \dots, b_{\Omega/\xi}^{\theta}\}$, where $b_{\Omega/\xi}^{\theta}$ is the θ th grid in the Ω/ξ distribution map. We consider the areas that always contain electric vehicles as candidate key areas, i.e., $P_{important}$. However, there are some $P_{important}$ areas that contain too few electric vehicles to reflect the application value of XFC stations that provide charging services in this area. Therefore, we need to select $P_{important}$ to obtain grids with high coverage and a stable number of EVs. To achieve this goal, we first calculate the average value of electric vehicles (i.e., E_i) contained in grid i in the Ω/ξ electric vehicle distribution map by Eq. (1).

$$E(i) = \frac{\sum_{j=1}^p a_{ij}}{p}, \quad (1)$$

where a_{ij} is the number of electric vehicles included in grid i , which is in the j th electric vehicle distribution map. p is the number of electric vehicle distribution maps, and $p = \Omega/\xi$.

We use variance as the main measure to explain the dynamic change process of electric vehicles in continuous time. In the Ω/ξ EV distribution maps, the average value of the number of EVs contained in all grids is averaged to obtain E_{mean} , as shown in Eq. (2). We require that the service areas of the selected XFC stations achieve not only large-scale EV coverage but also the stability of the number of EVs covered in this area. Therefore, it is necessary to exclude grids with a low variance but containing a small number of EVs, i.e., we need to exclude a class of grids that meet $E(i) < E_{mean}$. Then, we calculate the variance (i.e., S_i^2) of the EV number distribution of the remaining grids i by Eq. (3).

$$E_{mean} = \frac{\sum_{i=1}^{\theta} E(i)}{\theta}, \quad (2)$$

$$S_i^2 = \frac{(E(i) - a_{i1})^2 + (E(i) - a_{i2})^2 + \dots + (E(i) - a_{ij})^2}{j}. \quad (3)$$

We sort the obtained distribution variance S_i^2 from small to large and select the grid corresponding to the first L variances as the filtered key areas (i.e., $P_{important}$). As a result, a large number of electric vehicles are always distributed in $P_{important}$. Therefore, using the XFC station for charging in $P_{important}$ can improve the utilization rate of the XFC station.

3.2 Minimizing the number of XFC stations

In this paper, we consider the problem of maximizing the coverage of XFC stations based on minimizing the number of XFC stations. Under this optimization goal, electric vehicles in $P_{important}$ always show a dense distribution. As shown in Eq. (4), the service area D of the XFC station is further reduced in this area,

$$D = D_{\cap} \cup D_{al}, \quad (4)$$

where $D_{\cap} = \{D_{\cap 1}, D_{\cap 2}, \dots, D_{\cap s}\}$ represents the intersection of the range of all electric vehicles in $P_{important}$, and s represents the number of electric vehicles in $P_{important}$. The range of all electric vehicles in $P_{important}$ that do not have any intersection with any electric vehicle in the area can be obtained by Eq. (5). b represents the number of electric vehicles that do not have an intersection with any electric vehicle in $P_{important}$.

$$D_{al} = \{D_{al_1}, D_{al_2}, \dots, D_{al_b}\}. \quad (5)$$

As shown in Fig. 1, we use the node ID to construct the adjacency matrix. The value of the diagonal of the adjacency matrix is 0. If the driving ranges of the two nodes intersect,

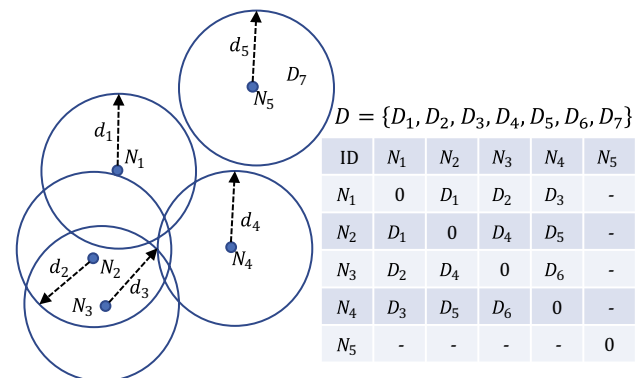


Fig. 1 Deployment area D identification diagram

the value is D_1 . If the driving ranges of the two nodes do not intersect, the value is represented by "-". We use 5 nodes to explain the deployment area D , of which $\{N_1, N_2\}$, $\{N_1, N_3\}$, $\{N_1, N_4\}$, $\{N_2, N_3\}$, $\{N_2, N_4\}$, and $\{N_3, N_4\}$ have intersections, which are D_1, D_2, D_3, D_4, D_5 , and D_6 . As a result, $D_\cap = \{D_1, D_2, D_3, D_4, D_5, D_6\}$. However, N_5 does not have an intersection with other nodes in the figure, whose scope is the deployment area D_7 , and $D_{at} = \{D_7\}$.

According to the calculation, the reduced deployment range D of the XFC station is a region set. For any element D_j in the set, we know the electric vehicle set G_j covered in the D region based on Eq. (6),

$$G_j = \bigcup_{i=1}^{|N|} \{i | d_i \cap D_j \neq \emptyset\}, \quad (6)$$

where $|N|$ is the total number of electric vehicles in the 2-dimensional area, and d_i is the range of electric vehicles N_i . According to Eq. (7), it can be seen that the set of electric vehicles in the deployment area together constitutes all the electric vehicles in the $P_{important}$ area,

$$G = \bigcup_{j=1}^{|D|} G_j. \quad (7)$$

For electric vehicles in the $P_{important}$ area, this paper defines a matrix of $|G| \times |D|$. These matrix elements are c_{ij} , which are obtained by Eq. (8),

$$c_{ij} = \begin{cases} 1 & i \in G_j \\ 0 & \text{otherwise} \end{cases}. \quad (8)$$

To determine the final deployment area, we define the binary decision variable x_j by Eq. (9),

$$x_j = \begin{cases} 1 & \text{if } D_j \text{ is the final deployment area} \\ 0 & \text{if } D_j \text{ is not the final deployment area} \end{cases}. \quad (9)$$

To solve the problem of maximizing the coverage of XFC stations based on the minimum number of XFC stations, the optimization function to minimize the number of XFC stations deployed in the $P_{important}$ area is shown in Eq. (10),

$$\min \sum_{j=1}^{|D|} x_j, \quad (10)$$

$$\text{Subject to } \sum_{j=1}^{|D|} c_{ij} x_j \geq 1, \quad (11)$$

where $i \in \{1, 2, \dots, |G|\}$, $j \in \{1, 2, \dots, |D|\}$, $x_j \in \{0, 1\}$, $c_{ij} \in \{0, 1\}$, and $|D|$ is the number of candidate deployment areas. As shown in Eq. (11), the constraint objective of the optimization function is to ensure that all electric vehicles in the $P_{important}$ area belong to the charging range of at least one XFC station. This problem is a binary integer linear programming problem and also an NP-hard problem [40]. Therefore, we solve the problem of maximizing XFC station

coverage with the minimum number of XFC stations based on a heuristic algorithm.

The essence of the maximum coverage of the XFC station is to find the minimum number of XFC stations in the $P_{important}$ area to ensure that all electric vehicles in the area are covered by the charging range of the XFC station. In this paper, the problem of maximizing the coverage of the XFC station is transformed into a clique partitioning problem with low complexity. The clique partitioning problem refers to finding the minimum number of cliques that can divide a graph. Each clique represents a certain set of vertices, and any two vertices in a clique are connected by edges. Therefore, an undirected graph $G(V, E)$ is constructed according to the distances of all electric vehicles in the $P_{important}$ region. Each vertex in the graph represents a point in the electric vehicle set G in the $P_{important}$ region. If the distance between two EVs does not exceed twice the driving range of the EV, then an edge is connected between these two points. The original problem can be transformed into an undirected graph composed of all electric vehicles in the $P_{important}$ region to find the minimum number of cliques that can divide the undirected graph by using clique partitioning. The clique partitioning problem is NP-hard. Many heuristic algorithms can obtain approximate solutions to this problem in linear time. We use the heuristic algorithm proposed by Tseng et al. [41] to solve this problem. The main steps of the heuristic algorithm are described as follows:

- 1) For an undirected graph $G(V, E)$, we first extract the pair of vertices (w_1, w_2) with the most common neighbors. If there are multiple vertex pairs with the same maximum number of common neighbors in the graph, then we select the vertex pairs with the fewest edges to delete. If the number of edges to be deleted for merging these vertex pairs is the same, then choose a vertex pair arbitrarily.
- 2) Combine the selected vertex pair (w_1, w_2) into one vertex w_1 .
- 3) Edge deletion. There are three types of edges to be deleted: a: the edge connected between w_1 and w_2 ; b: the edges corresponding to the vertices with smaller index numbers in w_1 and w_2 are deleted from the edges of the vertex pair connected to the common neighbor; c: if there is a vertex in the graph, and the vertex is connected to only one vertex in the vertex pair, then delete the edge. After the edges are deleted, the undirected graph is updated.
- 4) Repeat the above three steps on the new undirected graph until there are no edges in the graph.

In the above algorithm, the process of merging vertices is the construction process of different cliques. As shown in

Fig. 2 Example of clique partitioning process

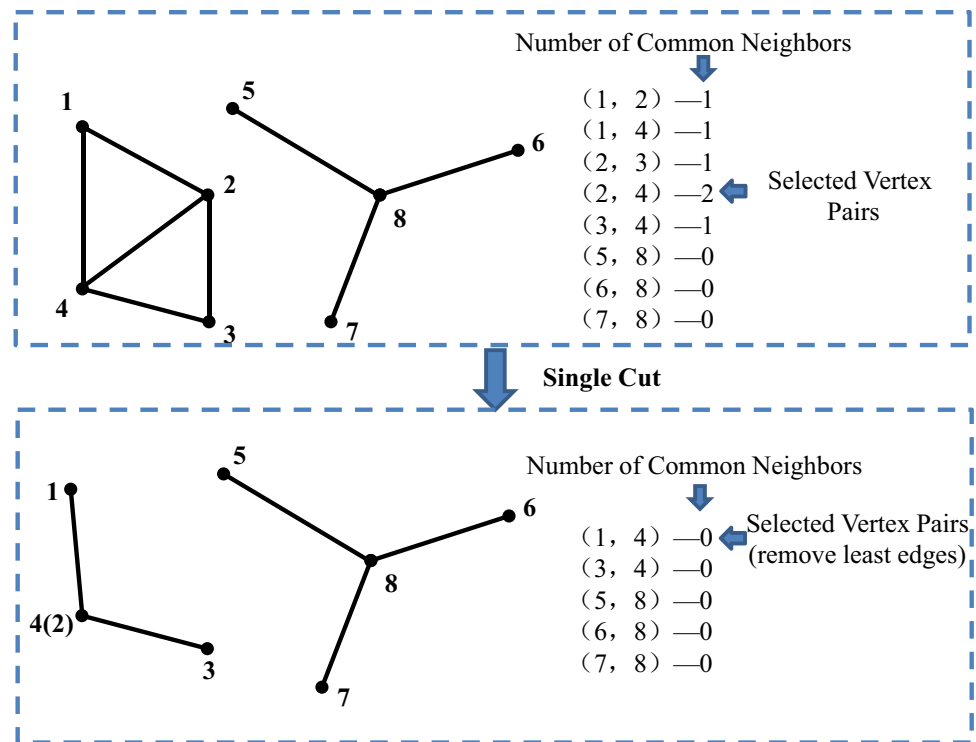


Fig. 2, we use an example to describe the clique partitioning algorithm. We first select the pair of vertices with the most common neighbors (2, 4) to merge and then delete the edges corresponding to the vertices with smaller index numbers to form a new undirected graph. In the new undirected graph, the common neighbors of all vertex pairs are zero, so the vertex pair with the fewest edges needs to be selected. This process is repeated until there are no edges in this graph. The original graph is divided into 5 cliques, which are $\{1, 2, 4\}$, $\{3\}$, $\{5, 8\}$, $\{6\}$, and $\{7\}$.

3.3 XFC station deployment optimization rules in the same clique

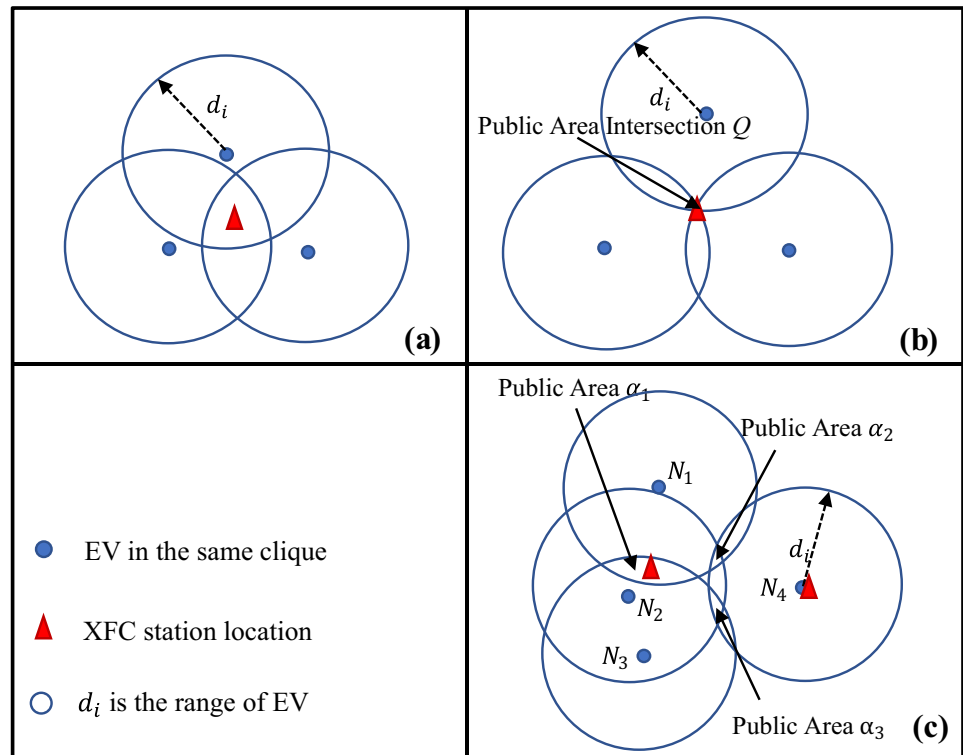
We consider that there are more complex intersections between the range of electric vehicles in a clique. To determine the specific deployment location of the XFC station, we optimize the specific deployment of the XFC station for three special situations to achieve the optimal deployment of the minimum number of XFC stations, thereby reducing the initial investment of the energy company. These rules can also minimize the overlapping coverage between XFC station service areas.

1) As shown in Fig. 3a, if the electric vehicles belonging to the same clique are in a unique public area, we consider the centroid of the unique public area as the deployment location of the XFC station.

2) There is a special situation where the scope of electric vehicles intersects, as shown in Fig. 3b. The scope of the three electric vehicles forms three public areas, and these 3 public areas intersect at one point. If we use the previous rule, two XFC stations will be deployed. However, for this situation, we can deploy the XFC station at the intersection Q of three public areas and replace the original two XFC stations with one, thereby reducing the number of XFC stations required.

3) As shown in Fig. 3c, there is no unique public area for electric vehicles belonging to the same clique. The four electric vehicles N_1, N_2, N_3 and N_4 intersect with each other. N_1, N_2 and N_3 have a unique public area α_1 , and electric vehicle N_4 does not intersect with the public area. In this case, if XFC stations are still deployed in the public area, three XFC stations are needed, namely, α_1 (i.e., public area of N_1, N_2, N_3), α_2 (i.e., public area of N_1, N_2, N_4) and α_3 (i.e., public area of N_2, N_3, N_4). We consider the deployment of XFC stations in the public areas α_2 and α_3 , which have a greater effect on electric vehicles N_4 and are not necessary for N_1, N_2 , and N_3 . Therefore, for this situation, we consider isolating one electric vehicle from the clique and then observing whether there is a unique public area for the remaining electric vehicles. If there is a unique public area, the XFC station will be deployed at the centroid of the unique public area and within the scope of the isolated electric vehicle. As shown in Fig. 3c, we first isolate the electric vehicle N_4 , find that N_1, N_2 and N_3 have a unique

Fig. 3 Schematic diagram of optimization rules



public area α_1 , and then deploy the XFC station at the centroid of α_1 and within the range of electric vehicle N_4 . We can simplify the three XFC stations originally needed to deploy two based on this rule. However, if the unique public area is not found after isolating one electric vehicle, we need to continue to select another electric vehicle for isolation and repeat the process until the unique public area is found.

3.4 Redetermining the XFC station deployment location

The optimization rules in Sect. 3.3 can be used to establish an equation for calculating the number of final XFC stations, as shown in Eq. (12)

$$XFCSNumber = Len(UPA) + Len(AN), \quad (12)$$

where $XFCSNumber$ represents the final number of charging stations. UPA represents the unique public area obtained through the deployment optimization rules of XFC stations in the same clique. $Len(UPA)$ is the number of unique public areas in the two-dimensional space. AN is a node that does not belong to any unique public area in a clique, which is defined as an alone node. $Len(AN)$ represents the number of alone nodes in the two-dimensional space.

For the alone node, the deployed charging station only needs to be within its scope. In contrast, for the unique

public area, we need to optimize the deployment location of the charging station. We know that the deployment location of the XFC station is the centroid of the area or the only intersection of the area in Sect. 3.3. We average the finite number of coordinates on the boundary of the unique public area to determine the centroid coordinates to obtain the deployment position of the XFC station in Eq. (13). We define this method as the Unique public area Location Method (ULM),

$$\begin{cases} CSLocationX = \begin{cases} \frac{\sum_{i=0}^{360} X_i}{360}, & CSNodeNumber > 1 \\ X_{Node}, & CSNodeNumber = 1 \end{cases} \\ CSLocationY = \begin{cases} \frac{\sum_{i=0}^{360} Y_i}{360}, & CSNodeNumber > 1 \\ Y_{Node}, & CSNodeNumber = 1 \end{cases} \end{cases}, \quad (13)$$

where $CSLocationX$ and $CSLocationY$ represent the abscissa and ordinate of the charging station respectively. $CSNodeNumber$ represents the number of nodes belonging to the current unique public area. If the unique public area belongs to only one node, the node coordinates (X_{Node}, Y_{Node}) are used to represent the deployment location of the XFC station. When the number of nodes belonging to the unique public area exceeds 1, there will be a unique public area in the clique. We divide the area boundary into 360 copies and calculate the average of the coordinates of the boundary points; then, the average position of the XFC station is $(\frac{\sum_{i=0}^{360} X_i}{360}, \frac{\sum_{i=0}^{360} Y_i}{360})$.

To further improve user satisfaction and the utilization of the XFC station, we optimize the total path length by minimizing the length of the path that each electric vehicle travels to the XFC station serving it, (i.e., there is an XFC station coordinate that satisfies the minimum total distance to the server node). We assume that the coordinates of the electric vehicle nodes are $(x_1, y_1), \dots, (x_n, y_n)$. The position of the charging station that satisfies the minimum total distance in the current unique public area can be obtained by Eq. (14) [42]. We name this method the Minimum distance sum Method (MM),

$$\min \sum_{i=1}^n \sqrt{(x - x_i)^2 + (y - y_i)^2}. \quad (14)$$

where x and x_i represent the abscissa of the electric vehicle. y and y_i represent the ordinate of the electric vehicle. MM can accurately find the target deployment location through Eq. (14), but its search speed will be affected by the search step size and search space size. Moreover, the deployment location of the XFC station determined by the ULM can only satisfy the deployment location of the XFC station within the unique public area. However, the ULM can obtain solutions quickly. Therefore, we combine the accurate MM with the fast ULM to determine the deployment location accurately and quickly. We define this method as the Minimum Distance Sum of a Unique Public area location (MISUP).

4 Experimental evaluation

4.1 Data initialization

This paper first verifies the method in Sect. 4.2 by using fewer than 200 randomly distributed EV nodes in $500 \text{ m} \times 500 \text{ m}$ area. In addition, we randomly distribute 4000 electric vehicles in $2000 \text{ m} \times 2000 \text{ m}$ area to verify our scheme in Sects. 4.3, 4.4, and 4.5. Then, we use MATLAB to generate 10 node topological maps to represent Ω/ξ electric vehicle distribution maps. The relationship between EVs also forms a network. In addition, the node topological map and the EV distribution map are mapped to each other, where Ω is the total evaluation time and ξ is the unit evaluation time. Different data are represented by the data ID. We use a square grid with a unit grid side length of $d = 100 \text{ m}$ to divide the node topological maps into integer grids. The range d_i of electric vehicles with the same remaining battery power and the charging range r_i of the XFC station are both $50\sqrt{2} \text{ m}$.

4.2 MDDC performance verification

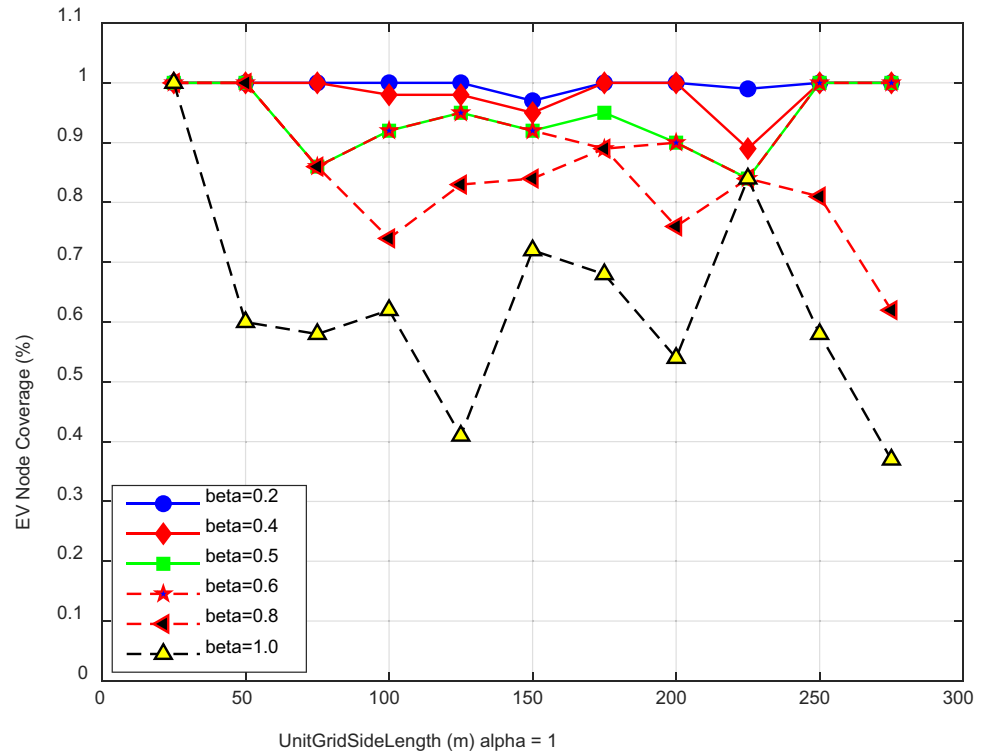
To ensure the rationality and validity of the experimental results, we use small-scale data to verify the performance

of the method in this paper. In the grid partitioning stage, to exclude a class of grids with a stable number of EVs but containing fewer EVs, the average EV contained in each grid in the Ω/ξ electric vehicle distribution maps is first calculated. Then, we average the averages of all the grids in the distribution maps and exclude the grids whose grid average $E(i)$ is less than the overall average E_{mean} (i.e., excluding a class of grid that meets $E(i) < E_{mean}$). However, excluding the grid may affect EV node coverage. Therefore, we introduce the factor $beta$ into the exclusion grid equation (i.e., $E(i) < beta * E_{mean}$) to evaluate the effect of the remaining grids on the coverage of the EV node to determine the optimal $beta$ value applicable in the current scenario. In this paper, we choose $beta = 1$. In addition, to determine that the selected grid has high stability, we calculate the variance of the remaining grids, sort them from small to large to select the first L grids as candidate XFC station service areas. Next, we introduce the factor $alpha$ to adjust the number of L (i.e., $L = alpha * N(RemainedGrid)$, where $N(RemainedGrid)$ is the number of remaining grids) to evaluate the effect of L on the coverage of EV nodes, so we can determine the optimal $alpha$ value suitable for the scene. As shown in Figs. 4 and 5, although $beta$ and $alpha$ are the same, the coverage under different unit grid side lengths usually changes. Therefore, we need to choose the appropriate unit grid side length during the partitioning process. In addition, as the value of $beta$ decreases, the node coverage rate increases. This is because as $beta$ decreases, the number of remaining grids gradually increases. However, when $beta$ is too small, we cannot exclude a grid that contains fewer EV nodes, so this cannot reflect the value of the XFC station. Therefore, it is very important to select a suitable $beta$. With the increase in $alpha$, the coverage of EV nodes shows an upward trend. The larger $alpha$ is, the more service areas are selected as candidate XFC stations, so we choose $alpha = 1$ for the next experiment.

Many heuristic algorithms can be used to solve the clique partitioning problem. However, there are differences in performance between different algorithms. Two heuristic algorithms proposed by Tseng et al. [41] and Khelldi et al. [43] were classic solutions used to solve the clique partitioning problem. Therefore, we need to evaluate them to determine which algorithm to choose as our solution. As shown in Fig. 6, the former is better than the latter in terms of the number of cliques and processing time, so we choose the former to solve the clique partitioning problem in this paper.

The MM is used to determine the points that satisfy the minimum distance sum of four points (i.e., $(0,0)$, $(50,0)$, $(50,50)$, and $(0,50)$) to evaluate the effect of the search step on the search time and error in a search space of size $50 \text{ m} \times 50 \text{ m}$. As shown in Fig. 7, as the search step length increases, the search time decreases rapidly and then flattens, while the error increases gradually and then increases

Fig. 4 The effect of unit grid side length and β on coverage



rapidly. Therefore, we know that choosing a reasonable search step is especially critical. When the search step size is 0.1, the search time and accuracy of the MM can be guaranteed. Therefore, the search step used in this paper is 0.1. In addition, we also evaluated the effect of search area

size on the MM. As shown in Fig. 8, as the search area increases, the search time of the MM search time increases rapidly. When the search area is too large, it will seriously affect the running efficiency of the program. Therefore, we consider optimizing the search space size of the MM

Fig. 5 The effect of unit grid side length and α on coverage

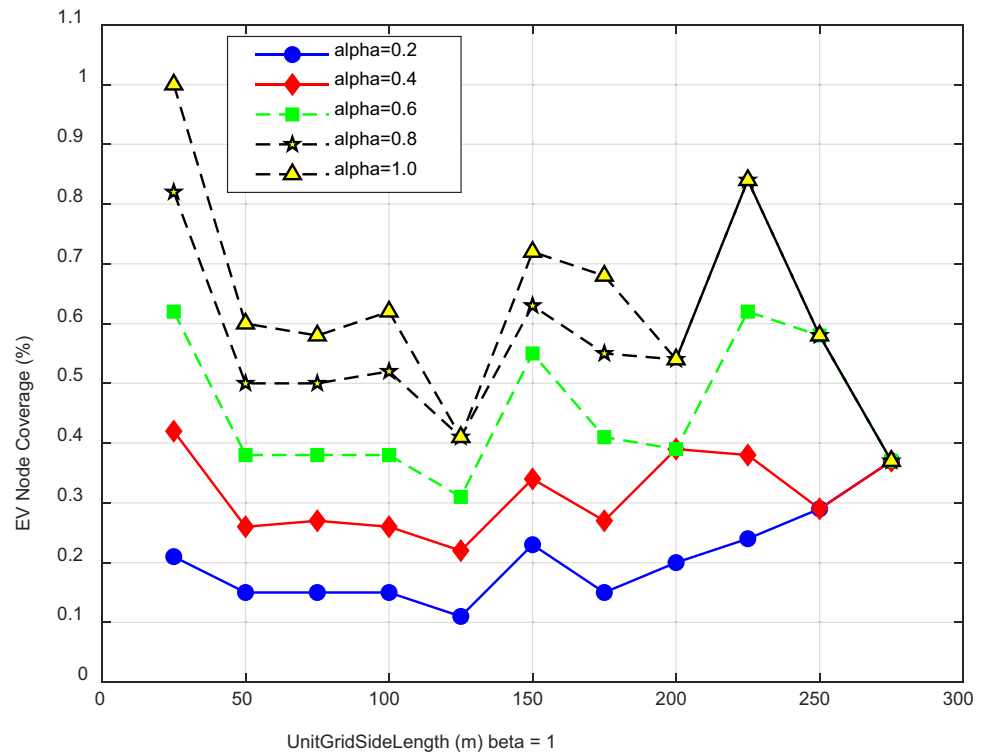
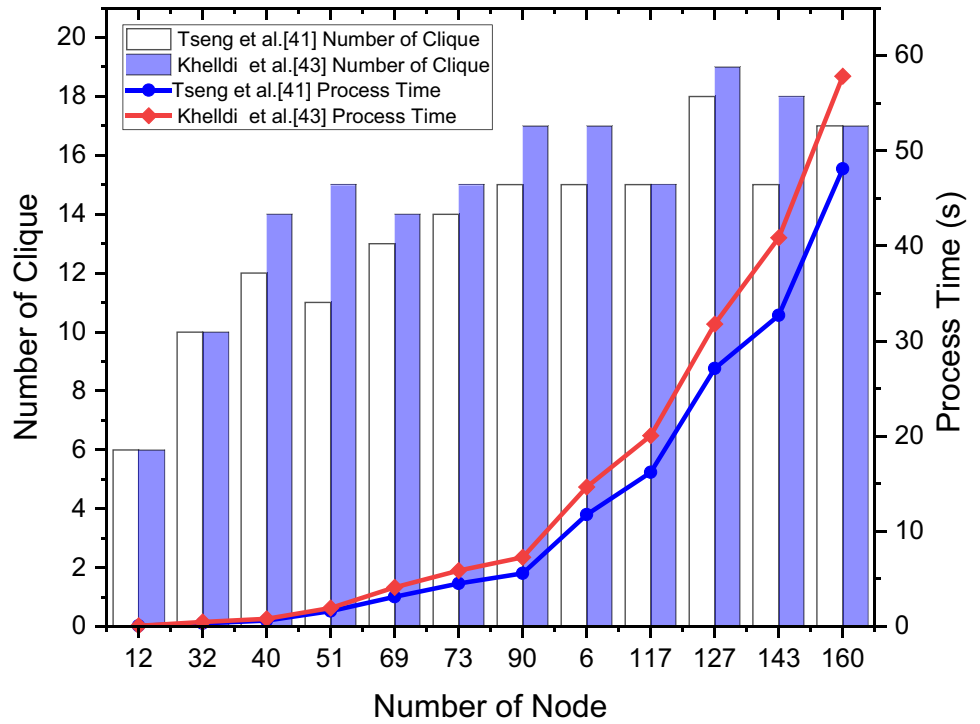


Fig. 6 Comparison of two heuristic algorithms



to reduce the algorithm search time. We consider combining the fast ULM and accurate MM to design the MISUP to overcome the shortcoming of slow MM search speed. We need to verify the performance of MISUP. As shown in Fig. 8, as the search space increases, the search time of MISUP does not increase significantly. Compared with the

MM, the search time of MISUP is greatly reduced. Therefore, we can use MISUP to obtain the XFC station deployment location that meets the conditions in a short time.

In addition, we use the GA to solve the optimal deployment location of the charging station [8]. The relevant parameter settings of the GA algorithm used are shown in

Fig. 7 Relationship between search time, error and search step

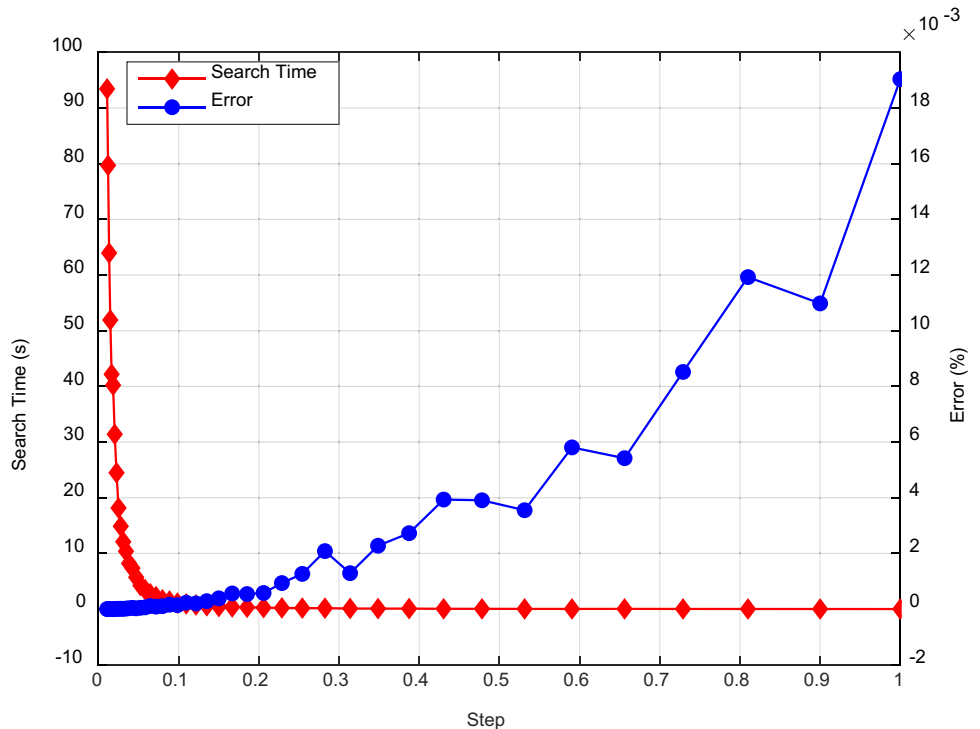


Fig. 8 Relationship between search space and search time

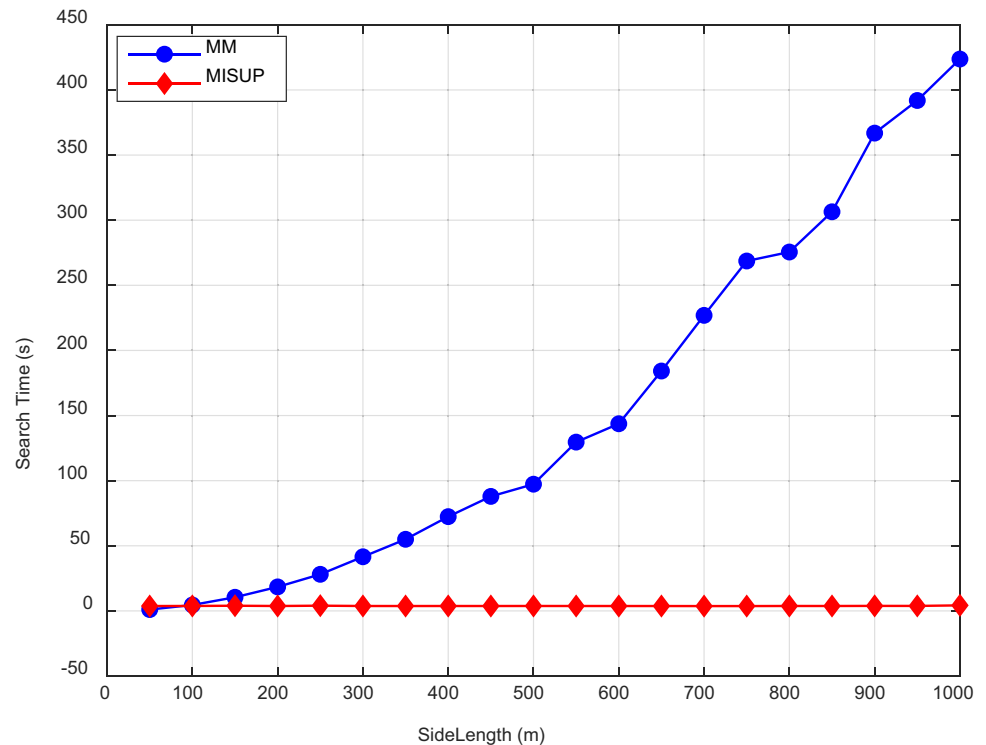


Table 1. The optimization results in this paper are coordinates, so two binary-encoded DNAs need to be defined, where one represents the abscissa and the other represents the ordinate. The GA is first evaluated in a $500\text{ m} \times 500\text{ m}$ search space. As shown in Fig. 9, after the genetic generation reaches 440 generations, the average and best fit results tend to be stable and approximately equal. This shows that the GA has found a solution that meets the conditions. Therefore, it only needs to iterate 440 generations to obtain appropriate results in the experiment.

To compare the performance of the MM, MISUP, and GA in the process of redetermining the position of the XFC station, we need to compile statistics on the final results. We first calculate the sum of the distance from each XFC station to the served node after processing. Then, we calculate the sum of the distances from all XFC stations in the two-dimensional space to the EVs they serve. As shown in Fig. 10, the results are obtained when the number of EV nodes is 80. The distance between XFC station IDs {1, 2, 3, 4, 5, 6} is small and equal. The result corresponds to the case of the alone node

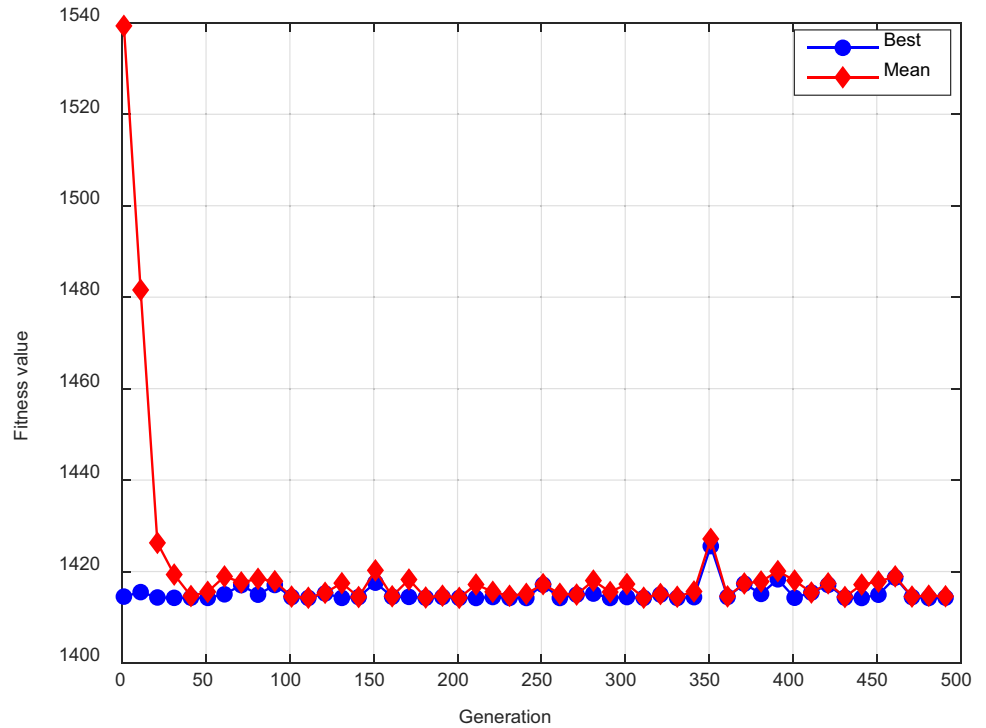
or the case where there is only one subordinate node in the unique public area. The other XFC station IDs correspond to the case where the number of subordinate nodes in the unique public area is greater than 1. It can be seen in the results that under the current conditions, the performance of MISUP is better than the other two methods, and the worst case is equal to the other two methods. As shown in Fig. 11, the results show that the distance sum generated by using MISUP is always less than or equal to the GA and ULM.

In the following, the performance of MDDC is verified, we use the Euclidean algorithm and the A-Star algorithm to calculate the distance between two nodes. We determine the relationship between the distance between two nodes and the radius of the range to which the EV node belongs (i.e., if the distance is less than 2 times the range radius, the return result is 1; otherwise, it is 0) and map the results to the adjacency matrix. We use heuristic algorithms to perform clique partitioning operations on the adjacency matrix to achieve the clustering of EV nodes. Then, we use the optimization rules in the same clique to process the clustering results to obtain the minimum number of XFC stations required. As shown in Fig. 12, using optimization rules in the same clique to optimize the results after clique partitioning processing can greatly reduce the number of XFC stations deployed and reflect the rationality and effectiveness of the rules. We evaluate the effect of different distance calculation methods on the results. The experiments show that under the influence of multiple factors, the final results have the same fluctuation trend and

Table 1 Related Parameters of GA

Parameter	Value
Population	100
Cross Probability	0.8
Mutation Probability	0.00
Search Space Size	$500\text{ m} \times 500\text{ m}$

Fig. 9 Relationship between the number of iterations and the fitness value



similar results, which shows that the method in this paper has good robustness. In addition, we compare our method (MDDC) with the method in Rajabi-Ghahnavieh et al. [37]. The obtained data were processed with tenfold cross-validation. The final results show that the performance before MDDC optimization is worse than the comparison, and the performance after MDDC optimization is better than the comparison. This is because the results before the optimization of the MDDC mainly consider achieving

full coverage of the nodes in the key area without focusing on overlapping coverage. The optimization goal in the comparison scheme is to minimize the cost and use genetic algorithms to solve the problem, so overlapping coverage can be reduced. However, we often obtain a locally optimal solution in the GA. In contrast, the optimization rules proposed in this paper can always eliminate the problem of overlapping coverage to the greatest extent, so the optimized MDDC can obtain the optimal results.

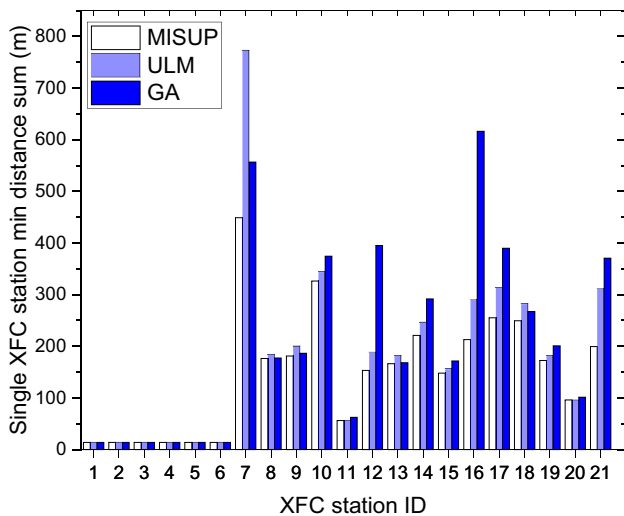


Fig. 10 Sum of distance from single XFC station to service node

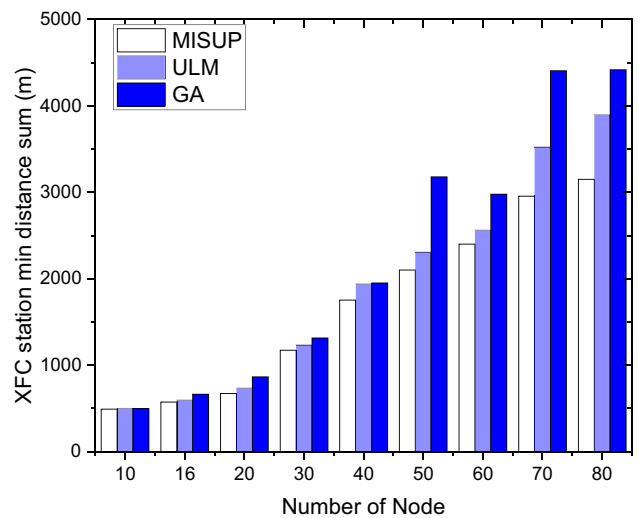
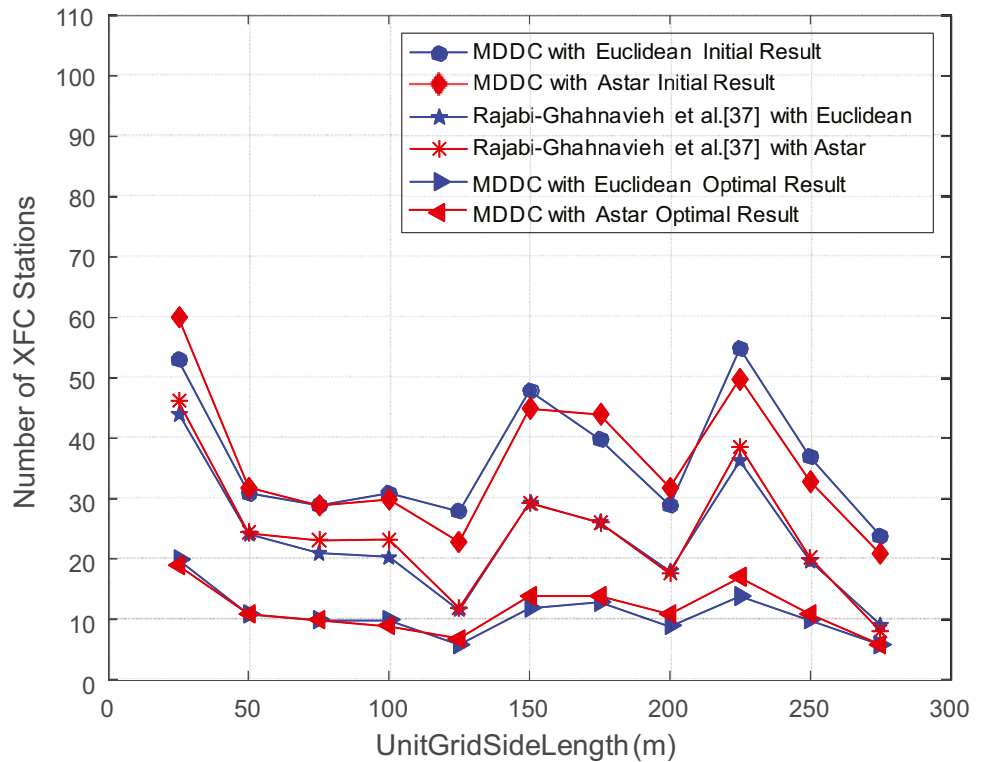


Fig. 11 The sum of the distance from all XFC stations to the EV nodes they serve

Fig. 12 Comparison of the number of XFC stations under different methods and scenarios using different calculations distance methods



4.3 Analysis of the minimum number of XFC stations required under different data types

We determine the $P_{important}$ area in different EV distribution maps under different data and construct the corresponding undirected graph. Then, we apply the MDDC method to find the minimum number of XFC stations required on different undirected graphs. As shown in Fig. 13, the minimum number of XFC stations required under different data is compared. We find that the number of XFC stations obtained under uniform distribution data is greater than the Poisson distribution and Gaussian distribution. This is because the EV distribution in the $P_{important}$ area for different data under the uniform distribution data is more scattered than the Poisson distribution and Gaussian distribution. Therefore, the number of edges in an undirected graph based on the range of electric vehicles in the uniform distribution is less than the Poisson distribution and Gaussian distribution, and the correlation between elements is not as strong as the Poisson and Gaussian distributions. Nodes with strong correlation will be divided into the same clique, so the number of XFC stations finally obtained from the data under uniform distribution is more than the Poisson distribution and Gaussian distribution. As shown in Fig. 14, the average number of XFC stations required under different data distributions shows that the Gaussian distribution is significantly lower than the uniform distribution.

4.4 Analysis of the feasibility of minimizing the XFC station optimization method

The clique partitioning algorithm can only divide electric vehicles into different cliques. The specific deployment location of the XFC station depends on the distribution of the electric vehicle. Taking data ID2 as an example, as shown in Fig. 15, the number of cliques obtained by applying the clique partitioning algorithm is much smaller than the number of XFC stations required before optimization based on the ID2 data, which obeys uniformly distributed data. This is because the distribution locations of electric vehicles in the same clique are complex, and there is an intersection between any two nodes. However, since the electric vehicles in the same clique are relatively scattered compared to the Poisson and Gaussian distributions, the elements are weakly related. As a result, it is difficult to find a unique public intersection to deploy the XFC station in a clique. Before the optimization, the XFC stations are deployed in all intersections existing in the same clique. Many common intersections belonging to the scope of multiple electric vehicles can be found, thereby reducing the number of XFC stations required by optimization. In the Poisson distribution and Gaussian distribution of data, the distributions of electric vehicles are highly correlated, and the number of cliques divided is less than the uniform distribution. For electric vehicles in the same clique, the probability of finding a common intersection belonging to the range of multiple electric

Fig. 13 Comparison of the minimum number of XFC stations required under different data types

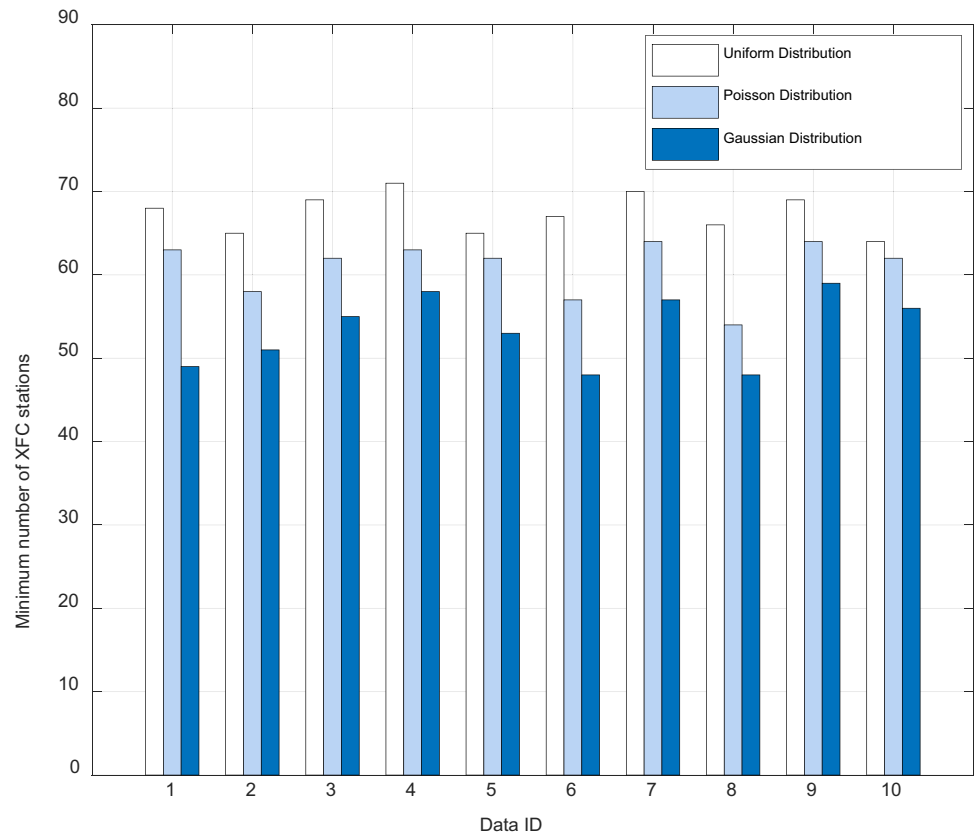


Fig. 14 Comparison of minimum required XFC station averages under different data types

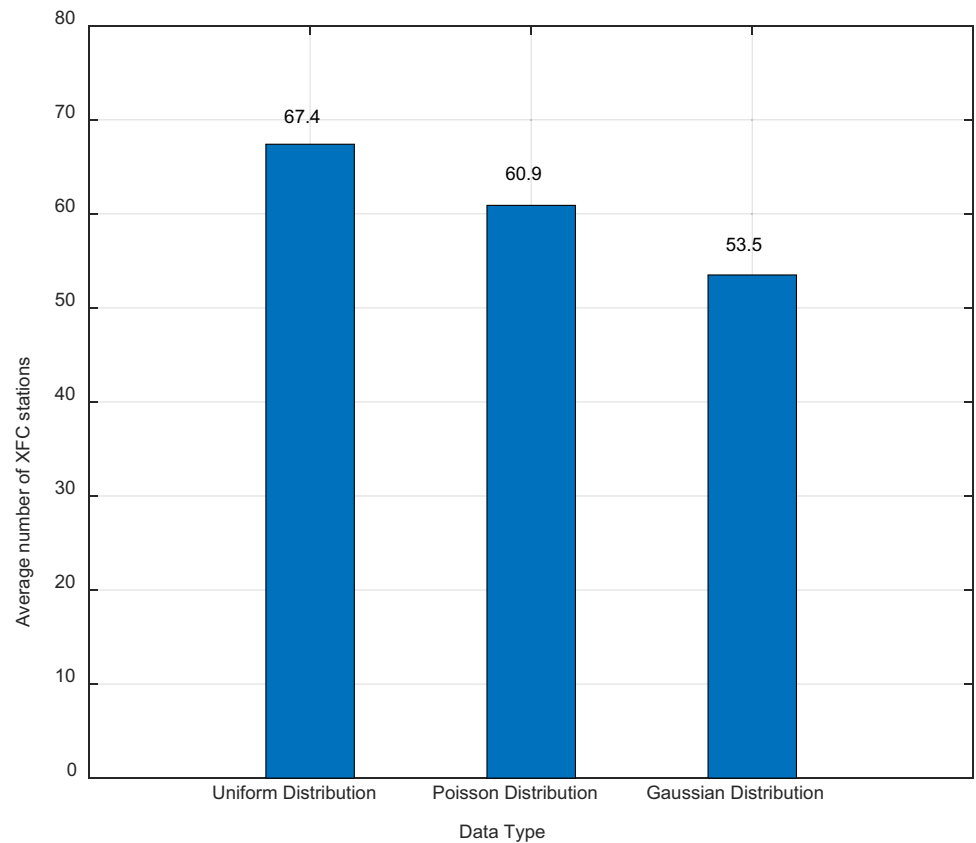
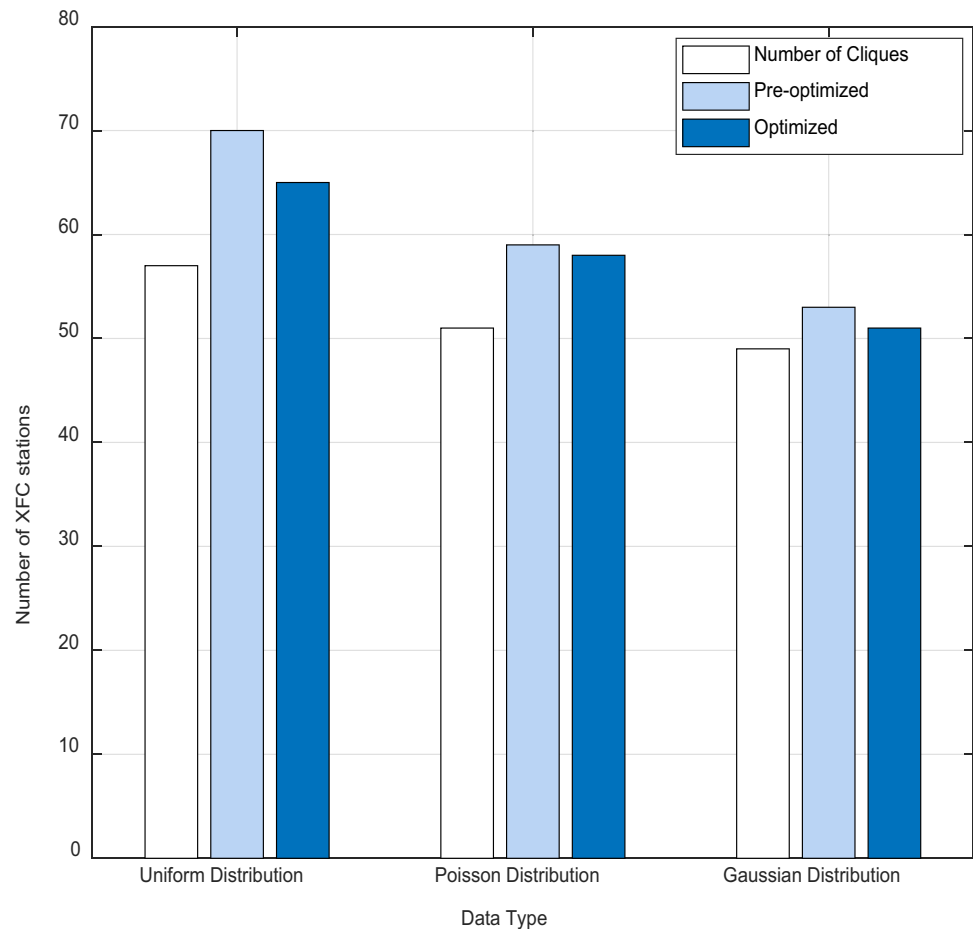


Fig. 15 Comparison of the number of XFC stations required before and after optimization



vehicles is large, so the number of XFC stations required before and after optimization does not change much.

4.5 Analysis of the impact of charging range r_i and the range d_i of EV based on minimizing XFC stations

The charging range r_i of the XFC station and the range d_i of the electric vehicle may affect the minimum number of XFC stations required. To verify the impact of these two factors on the results, we used uniformly distributed data to change the coverage of the XFC station and the range of electric vehicles to observe its impact on the minimum number of XFC stations required. As shown in Table 2, as the range of electric vehicles increases, the number of minimum required XFC stations gradually decreases, which indicates that the range d_i has a negative correlation with the number of minimum required XFC stations. At the same time, it can be seen that the larger the coverage area of the XFC station is, the fewer the minimum number of XFC stations required. This is because, with a larger coverage area for the XFC station, which can cover both the electric vehicles in the clique and a small number of electric vehicles in other cliques, the

impact on reducing the number of XFC stations is small. The method proposed in this paper is only applicable when $r_i \geq d_i$ since the core concept of the MDDC method is to convert the NP-hard problem into a clique partitioning problem. When constructing an undirected graph, the condition for constructing edges between any two nodes is that the nodes belong to the intersection range, which also determines that the structure of the undirected graph is affected

Table 2 The Influence of EV Range on Minimum Number of XFC Stations Required

EV Range d_i (m)	XFC Station Coverage $r_i = 50$ (m)	XFC Station Coverage $r_i = 70$ (m)
10	98	96
20	92	89
30	87	85
40	80	80
50	73	73
60	-	-
70	-	65

by the range d_i . If $d_i > r_i$, the deployment of the XFC station in the public area of the clique will not be able to cover all electric vehicles in the clique, which is unreasonable.

5 Conclusion

In this paper, we determine the locations of XFC stations based on the dynamic location change process of EVs. We first use ten electric vehicle distribution maps to approximate the dynamic location changes of EVs. The grid partitioning method is used to reduce the service area of the XFC station. An optimization function with a heuristic algorithm is designed to minimize the number of XFC stations required, which can determine the minimum number of XFC stations required to cover all electric vehicles in the service area of the XFC station. According to the range of EVs in the service area of the XFC stations, the XFC station deployment optimization rules are designed in the same clique, which can reduce overlapping coverage between XFC station service areas to optimize the XFC station deployment. In addition, to improve user satisfaction and the utilization of the XFC stations, we redetermined the deployment location of the XFC stations with the minimum distance sum as the optimization goal. MISUP is designed in the MDDC to accurately determine the target deployment location of the XFC stations in a short time. Finally, we verified the effectiveness, rationality, and robustness of the MDDC and evaluated its performance through simulation experiments. The results show that the MDDC outperforms the comparison algorithm by 54.2% and 52.0% when using the Euclidean algorithm and the A-star algorithm, respectively.

Funding This work was supported in part by the National Science Foundation of Hunan Province under Grant 2018JJ3692; by the National Science Foundation of Changsha City under Grant 63004; by the National Natural Science Foundation of China under Grant 61772559 and 62172443; by the Fundamental Research Funds for the Central Universities of Central South University (China) under Grant 2021zzts0735 and 2021zzts0753..

Declarations

Conflict of interest The authors declare that there is no conflict of interest regarding the publication of this paper.

References

- Xiong Y et al (2017) Optimal electric vehicle fast charging station placement based on game theoretical framework. *IEEE Trans Intell Transp Syst* 19(8):2493–2504
- Wang X et al (2016) Electric vehicle charging station placement for urban public bus systems. *IEEE Trans Intell Transp Syst* 18(1):128–139
- Fang C et al (2020) Dynamic pricing for electric vehicle extreme fast charging. *IEEE Trans Intell Transp Syst* 22(1):531–541
- Shareef H et al (2016) A review of the stage-of-the-art charging technologies placement methodologies and impacts of electric vehicles. *Renew Sustain Energy Rev* 64:403–420
- He J et al (2018) An optimal charging station location model with the consideration of electric vehicle's driving range. *Transp Res C Emerg Technol* 86:641–654
- Cao Y et al (2018) Toward distributed battery switch based electromobility using publish/subscribe system. *IEEE Trans Veh Technol* 67(11):10204–10217
- Zhang Y et al (2018) Optimal charging scheduling by pricing for ev charging station with dual charging modes. *IEEE Trans Intell Transp Syst* 20(9):3386–3396
- Efthymiou D et al (2017) Electric vehicles charging infrastructure location: a genetic algorithm approach. *Eur Transp Res Rev* 9(2):27
- Pinto F et al (2016) Space-aware modeling of two-phase electric charging stations. *IEEE Trans Intell Transp Syst* 18(2):450–459
- Iyer V et al (2018) Extreme fast charging station architecture for electric vehicles with partial power processing. In: 2018 IEEE Applied Power Electronics Conference and Exposition (APEC), San Antonio, TX, pp 659–665
- Liu Y et al (2019) Challenges and opportunities towards fast-charging battery materials. *Nat Energy* 4(7):540–550
- Chen X et al (2021) Enabling extreme fast charging technology for electric vehicles. *IEEE Trans Intell Transp Syst* 22(1):466–470
- Cui Q et al (2019) Electric vehicle charging station placement method for urban areas. *IEEE Trans Smart Grid* 10(6):6552–6565
- Davidov S, Pantoš M (2017) Planning of electric vehicle infrastructure based on charging reliability and quality of service. *Energy* 118:1156–1167
- Xiang Y et al (2016) Economic planning of electric vehicle charging stations considering traffic constraints and load profile templates. *Appl Energy* 178:647–659
- Gopalakrishnan R et al (2016) Demand prediction and placement optimization for electric vehicle charging stations. In: Proceedings of the Twenty-Fifth International Joint Conference on Artificial Intelligence, pp 3117–3123
- Zhao H, Li N (2016) Optimal siting of charging stations for electric vehicles based on fuzzy delphi and hybrid multi-criteria decision making approaches from an extended sustainability perspective. *Energies* 9(4):270
- Zhang Y et al (2019) Expanding ev charging networks considering transportation pattern and power supply limit. *IEEE Trans Smart Grid* 10(6):6332–6342
- Yang W et al (2020) Joint planning of ev fast charging stations and power distribution systems with balanced traffic flow assignment. *IEEE Trans Ind Inf* 17(3):1795–1809
- Luo C et al (2015) Placement of ev charging stations—balancing benefits among multiple entities. *IEEE Trans Smart Grid* 8(2):759–768
- Wu X et al (2021) A novel fast-charging stations locational planning model for electric bus transit system. *Energy* 224:120106
- Andrenacci N et al (2016) A demand-side approach to the optimal deployment of electric vehicle charging stations in metropolitan areas. *Appl Energy* 182:39–46
- Vazifeh M et al (2019) Optimizing the deployment of electric vehicle charging stations using pervasive mobility data. *Transp Res Part A Policy Pract* 121:75–91
- Wei W et al (2017) Expansion planning of urban electrified transportation networks: a mixed-integer convex programming approach. *IEEE Trans Transport Electrif* 3(1):210–224
- Wang S et al (2018) Stochastic collaborative planning of electric vehicle charging stations and power distribution system. *IEEE Trans Ind Informat* 14(1):321–331
- de Quevedo P et al (2019) Impact of electric vehicles on the expansion planning of distribution systems considering

- renewable energy storage and charging stations. *IEEE Trans Smart Grid* 10(1):794–804
27. Zhang H et al (2017) Optimal planning of pev charging station with single output multiple cables charging spots. *IEEE Trans Smart Grid* 8(5):2119–2128
 28. Chen H et al (2019) Design and planning of a multiple-charger multiple-port charging system for pev charging station. *IEEE Trans Smart Grid* 10(1):173–183
 29. Yang Q et al (2019) Optimal sizing of pev fast charging stations with Markovian demand characterization. *IEEE Trans Smart Grid* 10(4):4457–4466
 30. Liu X et al (2022) Time efficient tag searching in large-scale rfid systems: a compact exclusive validation method. *IEEE Trans Mob Comput* 21(4):2891–2905
 31. Liu X et al (2021) Time-efficient target tags information collection in large-scale rfid systems. *IEEE Trans Mob Comput* 20(4):2891–2905
 32. Xue Y et al (2016) Adopting strategic niche management to evaluate ev demonstration projects in china. *Sustainability* 8(2):142
 33. Aljaidi M (2019) Optimal placement and capacity of electric vehicle charging stations in urban areas: survey and open challenges. In: 2019 IEEE Jordan International Joint Conference on Electrical Engineering and Information Technology (JEEIT), pp 238–243
 34. Zhu Z et al (2018) Charging station planning for plug-in electric vehicles. *J Syst Sci Syst Eng* 27(1):24–45
 35. Alhazmi Y et al (2017) Optimal allocation for electric vehicle charging stations using trip success ratio. *Int J Electr Power Energy Syst* 91:101–116
 36. Li J et al (2018) Planning electric vehicle charging stations based on user charging behavior. In: 2018 IEEE/ACM Third International Conference on Internet-of-Things Design and Implementation (IoTDI), pp 225–236
 37. Rajabi-Ghahnavieh A, Sadeghi-Barzani P (2016) Optimal zonal fast-charging station placement considering urban traffic circulation. *IEEE Trans Veh Technol* 66(1):45–56
 38. Ge S et al (2012) The planning of electric vehicle charging stations in the urban area. In: 2nd International Conference on Electronic & Mechanical Engineering and Information Technology, pp 1598–1604
 39. Sadeghi-Barzani P et al (2014) Optimal fast charging station placing and sizing. *Appl Energy* 125:289–299
 40. Karp R (1972) Reducibility among combinatorial problems. In: Miller RE, Thatcher JW, Bohlinger JD (eds) *Complexity of Computer Computations*. Springer, Boston, pp 85–103
 41. Tseng C, Siewiorek D (1986) Automated synthesis of data paths in digital systems. *IEEE Trans Comput Aided Des Integr Circuits Syst* 5(3):379–395
 42. Wang Q et al (2017) Optimized charging scheduling with single mobile charger for wireless rechargeable sensor networks. *Symmetry* 9(11):285
 43. Khelladi L et al (2017) Efficient on-demand multi-node charging techniques for wireless sensor networks. *Comput Commun* 101:44–56

Publisher's Note Springer Nature remains neutral with regard to jurisdictional claims in published maps and institutional affiliations.



Ping Zhong, Member, IEEE received her Ph.D. degree in Communication Engineering from Xiamen University, China, in 2011. She is currently an Associate Professor with the Department of Computer Science and Technology at Central South University. Her research interests include machine learning, data mining, and networks protocol design. She is a member of ACM, CCF, IEICE and IEEE.



Aikun Xu is currently a master student in the School of Computer Science and Engineering, Central South University, Changsha, China. He received the B.S. degree in the School of Computer Science from South Central University for Nationalities, Wuhan, China, in 2019. His research interests include machine learning, scheduling, electric vehicles, and wireless networks.



Yilin Kang received the Ph.D. degree in computer science from the Nanyang Technological University, Singapore. She is currently an Assistant Professor with the School of Computer Science, South-Central University for Nationalities, China. Her current research interests include human-centric computing, brain-inspired intelligent agent, cognitive and neural systems and human-computer interaction. Prior to joining SCUN, she was a research fellow with the NTU-UBC Joint Research Centre of Excellence in Active Living for the Elderly (LILY). She serves as PC members of AAAI 2020, AAAI 2019, IJCAI 2016 and OC members of IEEE WI/IAT 2015. She serves as reviewer in several major journals, such as IEEE trans. on NNLS, IEEE trans. on SMC and JAAMAS.



Shigeng Zhang, Member, IEEE received the B.Sc., M.Sc., and D. Eng. degrees in computer science from Nanjing University, Nanjing, China, in 2004, 2007, and 2010, respectively. He is currently an Associate Professor with the School of Computer Science and Engineering, Central South University, Changsha, China. His research interests include Internet of Things (IoT), mobile computing, RFID systems, and IoT security. Prof. Zhang is on the Editorial Board of International

Journal of Distributed Sensor Networks, and was a program committee member of many international conferences including IEEE International Conference on Communications, International Conference on Parallel and Distributed Systems, IEEE International Conference on Mobile Ad-Hoc and Smart Systems, IEEE International Conference on Ubiquitous Intelligence and Computing and IEEE International Symposium on Parallel and Distributed Processing with Applications. He has authored/coauthored more than 50 technique papers in top

international journals and conferences including Infocom, IEEE International Conference on Network Protocols, IEEE Transactions on Mobile Computing, IEEE Transactions on Computers, IEEE Transactions on Parallel and Distributed Systems, ACM Transactions on Sensor Networks, and IEEE Journal on Selected Areas in Communications. He is a member of ACM.



Yiming Zhang received the B.Sc. and M.Sc. degrees in mechanics engineering and the Ph.D. degree in Computer Science from the National University of Defense Technology (NUDT), Changsha, China, in 2001, 2003, and 2008, respectively. He is currently an Associate Professor with the School of Computer, NUDT. His current research interests include cloud-computing, machine learning, and networking. He received the China Computer Federation Distinguished Ph.D. Dissertation Award in 2011.